Robust optimization of an organic Rankine cycle for geothermal application

Aldo Serafino, Benoit Obert, Léa Vergé, Paola Cinnella

Version of Record: https://www.sciencedirect.com/science/article/pii/S0960148120311289
Manuscript_925083c52ab42032ecdffc3118a159bb

ROBUST OPTIMIZATION OF AN ORGANIC RANKINE CYCLE FOR GEOTHERMAL APPLICATION

Aldo Serafino [a,b] *, Benoit Obert [a], Léa Vergé [a], Paola Cinnella [b]

[a] *Enertime, 1 rue du Moulin des Bruyères, 92400 Courbevoie, France*
[b] *Laboratoire Dynfluid, Arts et Métiers ParisTech, 75013 Paris, France*

Abstract

A robust design optimization (RDO) methodology for Organic Rankine Cycles (ORC) is presented, allowing to ensure an improved, stable performance over a large range of operating conditions. In contrast with classical ORC design methods, whereby all modeling hypotheses and operating conditions are considered as perfectly known, i.e. deterministic, the RDO approach allows to account for the manifold sources of uncertainty affecting the system. For geothermal ORC, the latter are related on one hand with the ill-known properties of the geothermal source and, on the other, with intrinsically random parameters, such as the condensation temperature. The proposed RDO approach selects values of the design parameters that maximize the expected (average) performance while minimizing its variance under uncertain nominal operating conditions. The optimal design delivered by the proposed strategy outperforms the one derived from the standard deterministic approach: specifically, the expected power output is increased by 1.5%, while its standard deviation is reduced by 8.5% and the surface of the heat exchangers by 34%.

Keywords: Organic Rankine cycle, design methodology, optimization under uncertainty, robust design optimization, surrogate models

*aldo.serafino@enertime.com, aldo.serafino@ensam.eu

1. Introduction

The development of Organic Rankine Cycles (ORCs) in the last fifteen years has contributed significantly to the enlargement of the commercial exploitation of geothermal power. Specifically, the ORC technology has fostered the use of low-temperature geothermal resources. Data collected by Bertani [1, 2] show a noticeable growth in the worldwide installed geothermal capacity of binary plants (almost exclusively based on ORC technology), which in just 5 years has almost doubled passing from 11% to 14.2% of the overall geothermal applications. Among the 780 MW of new geothermal capacity installed in 2016 [3], almost 30% consists in ORC systems [4].

However, even if nowadays geothermal power is a mature, commercially available and well known technology providing low-cost base load capacity, several sources of uncertainty are hidden in the whole process adopted for its exploitation. Some major sources of epistemic uncertainties in geothermal power generation [5] are listed below:

- temperature of the geothermal reservoir;
- field extent for the definition of the drilling area;
- soil permeability;
- average well production;
- re-injection cost;
- phenomena like quenching, chemical clogging and corrosion.

Among them, just a few can be reduced, investing a considerable amount of time and capital resources in preliminary discovery and exploration activities, while some others can be reduced only through long term operation of the field (about a decade, as an order of magnitude). All of them are due to a lack of knowledge, and for that reason they are qualified as "epistemic" uncertainties [6, 7].

A large amount of literature has been written since the 70s to identify the sources of uncertainty affecting geothermal power and to quantify their effects. A detailed overview can be found for instance in [8]. These sources of uncertainty can lead to the scenario presented in Fig. 1, showing that

from an investor viewpoint a geothermal project can be a risky and capital-intensive investment. The risk derives from the fact that an important part of the capital is required for preliminary activities like pre-survey, exploration and test drilling without any certainty about the presence of an exploitable geothermal resource. For instance, the test drilling can account alone for up to 15% of the overall capital cost [9], before that the project profitability can be determined. Moreover, these sources of uncertainty can result in the oversizing of the geothermal plant, with a significant reduction of profits and a possible failure of the whole geothermal project. Considering that, historically, the majority of the worldwide geothermal installed capacity has been funded mainly through private financing [10], such a scenario can deter investments in this technology.

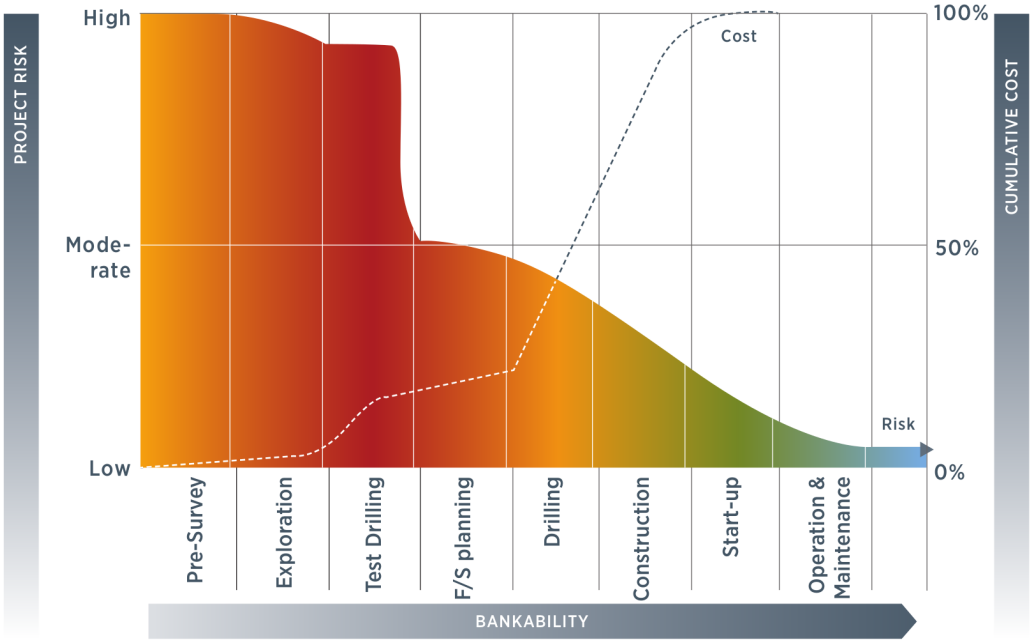

Figure 1: Typical uncertainty and expenditure profiles for a geothermal project [3]

Even if there is no reason to believe that the uncertainty and the risk associated with geothermal fields are any greater than those for other forms of electricity generation [5], the accurate quantification of geothermal resource risk is of a paramount importance in the financing of geothermal projects [11]. The objective of the present work is to employ a promising methodology aiming to perform the robust design optimization (RDO) of an ORC for a

geothermal application, which can take into account all these uncertainties in order to reduce the associated risk.

ORC design typically relies on a mathematical model of the cycle, allowing to evaluate a set of performance parameters (or cost functions) given a set of design variables. The model is supposed to provide an accurate enough description of the ORC system over a range of operating conditions. Several examples of thermodynamic and techno-economic optimization can be found in [12]. Historically, a black-box strategy has been typically applied, whereby the cycle performance is computed with a simulation code, while the design parameters are optimized with an evolutionary algorithm (e.g. simulated annealing, particle swarm, artificial bees colony or genetic algorithms); some examples can be found in [13, 14, 15, 16, 17, 18, 19]. For several years, the analysis has been carried out solely at a fixed design point, corresponding to the nominal working conditions of the ORC plant. Only recently some thermodynamic and techno-economic optimizations have been carried out considering also part-load performance: a first contribution has been given by [20]. Other interesting applications can be found in [21, 22, 23, 24, 25, 26, 27, 28]. Part-load performance is evaluated by means of dynamic simulations [12] or, more often, through steady state calculations at off design conditions [27]. In all cases, the optimization process is deterministic in the sense that the design variables, the operating conditions and any other input required by the model, as well as the model itself, are supposed as perfectly known.

However, due to epistemic and aleatory uncertainties in the operating conditions (as discussed in the above), the values to be input to the code are more properly described as random variables. Consequently, the performance of the system, which is obtained as the model output, is also random. An essential step is therefore to estimate the probability distribution function (PDF) describing the random variations of performance parameters. Such information can subsequently be used in the process to design ORCs with a controlled performance uncertainty. Design strategies for the optimization of a system subject to uncertainties are known as robust design optimization (RDO) methods [29]. Several RDO strategies exist, e.g. [30, 31, 32].

In this work, we focus on Taguchi's RDO approach [30], which looks for the maximization (or, depending on the problem, minimization) of the expectancy of a set of cost functions while minimizing at the same time their variances, thus reducing the sensitivity of the optimal design to uncertain parameters. For that purpose, the uncertain input parameters are assigned probability distributions, and an uncertainty quantification (UQ) method is

used to propagate them through a mathematical model of the system and to obtain the expected (average) values and the standard deviations of the output performance parameters (the cost functions). The UQ algorithm is then coupled with a multi-objective optimizer, allowing to determine the optimal designs with respect to the multiple cost functions.

In the context of ORC design under uncertain operating conditions, RDO represents a promising alternative to standard design methods [33], allowing to ensure a more stable performance over a range of randomly varying operating conditions.

The paper is presented as follows: Section 2 presents the ORC model employed in the calculations; Sections 3 and 4 describe the UQ methodology and the proposed RDO loop, respectively. Numerical results are presented in Section 5 and Section 6. Final remarks and conclusions are provided in Section 7.

2. ORC model

The object of the RDO carried out in this study is an ORC for geothermal application, whose plant layout is depicted in Fig. 2.

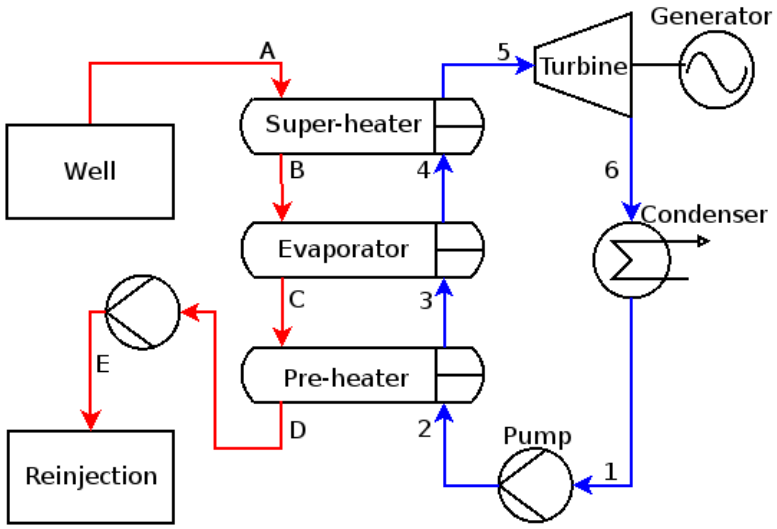

Figure 2: Layout of the geothermal plant

The plant exploits geothermal brine in a single-pressure ORC employing iC4 as the working fluid. As depicted in Fig. 2, the brine is cooled-down

before the re-injection by a set of heat exchangers (HEXs). These include a pre-heater (PRE), an evaporator (EVA) and, eventually, a super-heater (SH) where heat is transferred to the ORC working fluid. The PRE is a shell and tube heat exchanger, while the EVA is a kettle reboiler. The vapour of the working fluid, which can be saturated or superheated (depending on the outcomes of the RDO), expands in an axial turbine directly connected with the generator by means of a coupling disc. The condenser (CD) is a shell and tube heat exchanger using water, which is cooled in a wet cooling tower to condensate the vapour coming from the discharge of the turbine. Finally, the pump is of the centrifugal type and it is connected to an electrical driver equipped with a variable-frequency drive.

An in-house deterministic model for ORC systems written in Python is used for the design and the off-design simulation of the cycle, described in [34]. A brief overview of both design and simulation algorithms is provided hereafter for completeness.

The design algorithm, which is sketched in Fig.3, defines the proper size of all ORC components, in order to evaluate the performance and the cost of the whole system. Therefore, first the nominal operating conditions of the cycle should be assigned; these include the characteristics of both hot and cold energy sources and, more specifically, the nominal temperature, mass flow rate and specific heat capacity of the geothermal brine, the brine re-injection temperature (which is fixed at 353.15 K, to avoid corrosion and deposition issues), the inlet temperature and the mass flow rate of the cooling water. Additional inputs required by the model are:

- the subcooling,
- the superheating (ΔT_{SH}),
- the isentropic efficiency of the turbine,
- the efficiency of the pump,
- the pressure drops across the HEXs,
- the pinch points in the evaporator and in the condenser.
- the working fluid.

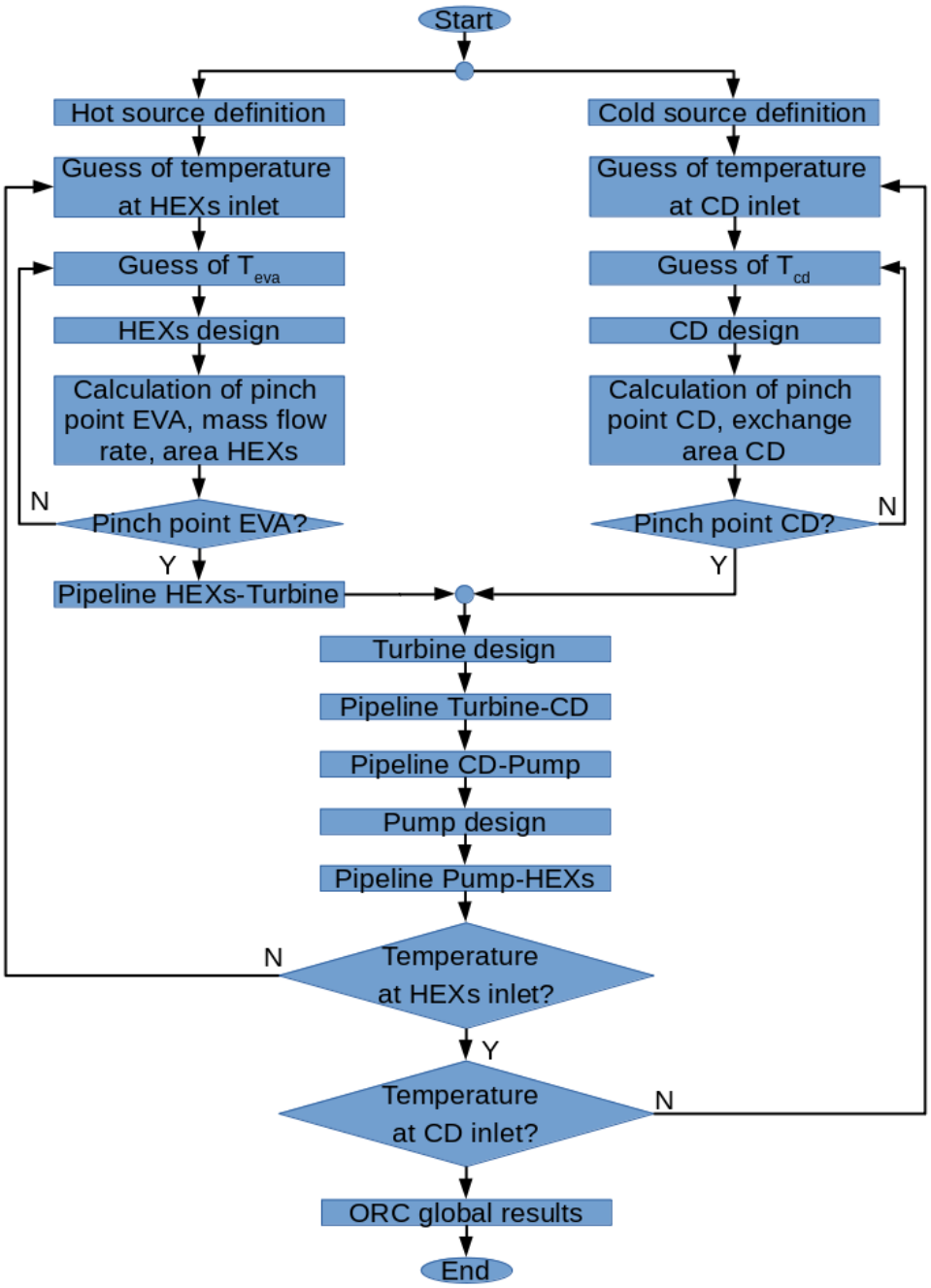

Figure 3: Flowchart of the ORC model in design mode (nominal conditions).

The turbine is designed to perform 85% isentropic efficiency at the design point, while the pump is chosen with a 70% overall efficiency. The PRE, the EVA and the SH (considered all together as a single block of HEXs) and the condenser are modelled with the generalized moving-boundary algorithm proposed in [35]; the ϵ-NTU method [36] is then used to estimate the exchange area at the ORC nominal point. Moreover, in order to have in the evaporator only the change of phase of iC4, a subcooling of 0.5 K of the working fluid is considered at the EVA inlet. The thermodynamic properties of the working fluid are calculated via the Coolprop 6.1.0 library [37].

Following the algorithm in Fig.3, once that both hot and cold sources are specified, the model can start with the design of the HEXs and of the condenser, which requires an initial guess of the temperature of the working fluid at the inlet of the condenser and of the HEXs block, as well as of the evaporator and condenser temperatures (respectively, T_{eva} and T_{cd}). The input data presented in Fig.4 are used to model the condenser and the HEXs. As an output of the design of these components, an estimation of the exchange areas, of the ORC mass flow rate and of the pinch points in the EVA and the condenser is provided; these two last quantities are used to check the pinch point values set at the beginning.

If the calculated pinch point values do not match to the fixed ones, a new guess of T_{eva} and T_{cd} is considered and a new run is performed. In the code, this iterative search of the roots is carried out with the Nelder-Mead algorithm [38] implemented in the Python library Scipy [39]. Once that the pinch-point values have been converged to within a tolerance of $10^{-4}K$, the algorithm proceeds with the design of the turbine, of the pump and of the pipelines between each item. The input data used for the design of each component are also listed in Fig.4. For the pipelines, a target pressure drop is imposed and the pipe diameters are calculated using the Colebrook-White correlation [40].

Before the end of the design, a check on the temperature of the working fluid at the inlet of the condenser and of the HEXs block is done: if the calculated values differ from the initial guess by more than $10^{-4}K$, these quantities are updated and a new run of the code is performed. When the convergence is reached, the design model outputs a list of parameters corresponding to the characteristics of the ORC. Tab.1 shows typical results for the design of an ORC.

Thus, the ORC model is first applied in the so-called design mode, to select the ORC design providing the best deterministic performance, at pre-

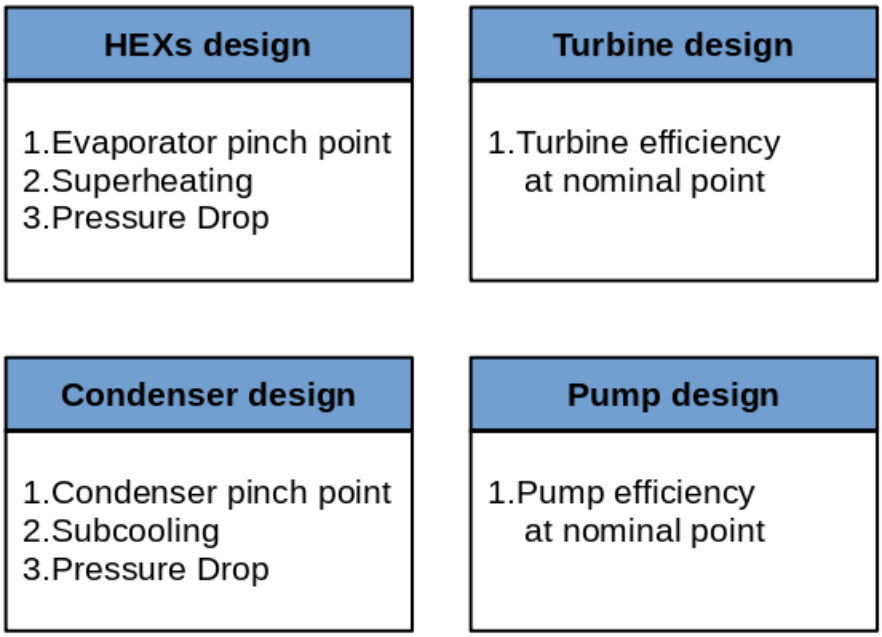

Figure 4: Input data for the design of the main components of the ORC at nominal conditions

specified nominal design conditions. The ORC off-design performance is then evaluated by running the model in the simulation mode, illustrated in the flowchart of Fig.5.

The hot and the cold sources are assigned for off design operating conditions: these include the mass flow rate, inlet temperature and specific heat capacity of the geothermal brine, and the inlet temperature and mass flow rate of the cooling water. A first guess for T_{eva} and T_{cd} is used to define the thermodynamic state at the inlet of the turbine and of the pump; pressures at the outlet of both components are also calculated. The input parameters of Fig.6, along with empirical correlations given by Enertime are used to calculate the pump and turbine off-design isentropic efficiencies. The turbine simulation allows to compute the ORC mass flow rate; with this last piece of information, one can simulate the pipelines between the turbine and the condenser and the one between the pump and the HEXs, obtaining an estimation of pressure drops in each line knowing its own diameter. Furthermore, the HEXs and the condenser can be also simulated: the same generalized moving-boundary algorithm already employed in the design mode, is now

Table 1: Some major results from the ORC design module

#	**Results from the ORC design module**
1	ORC mass flow rate
2	Pressure at evaporator (P_{eva})
3	ΔT_{SH}
4	Turbine Inlet Pressure
5	Turbine Outlet Pressure
6	Pressure at condenser (P_{cd})
7	Thermodynamic points of the ORC @ nominal point
8	Pump mechanical power
9	Cooling water mass flow rate
10	Thermal power input
11	Turbine mechanical power
12	Turbine electric power
13	ORC net power ($W_{ORC,net}$)
14	ORC efficiency
15	Exchange area of PRE
16	Exchange area of EVA
17	Exchange area of SH
18	Exchange area of CD
19	Diameter of the pipe between EVA and turbine
20	Diameter of the pipe between CD and pump
21	Diameter of the pipe between turbine and CD
22	Diameter of the pipe between pump and EVA

used to define the thermodynamic state at the boundaries and inside the HEXs block and the condenser, while the ϵ-NTU method is still utilized to compute the exchange area of both these two items. Finally, the areas of the HEXs and of the condenser are used to check convergence: if the values calculated in the simulation mode differ from the design values at nominal conditions by more than 10^{-6} m^2, a new guess value of T_{eva} and T_{cd} is considered and a new run is performed. To iterate through T_{eva} and T_{cd} the multi-objective COBYLA optimization algorithm [41] available in the Python library Scipy is used.

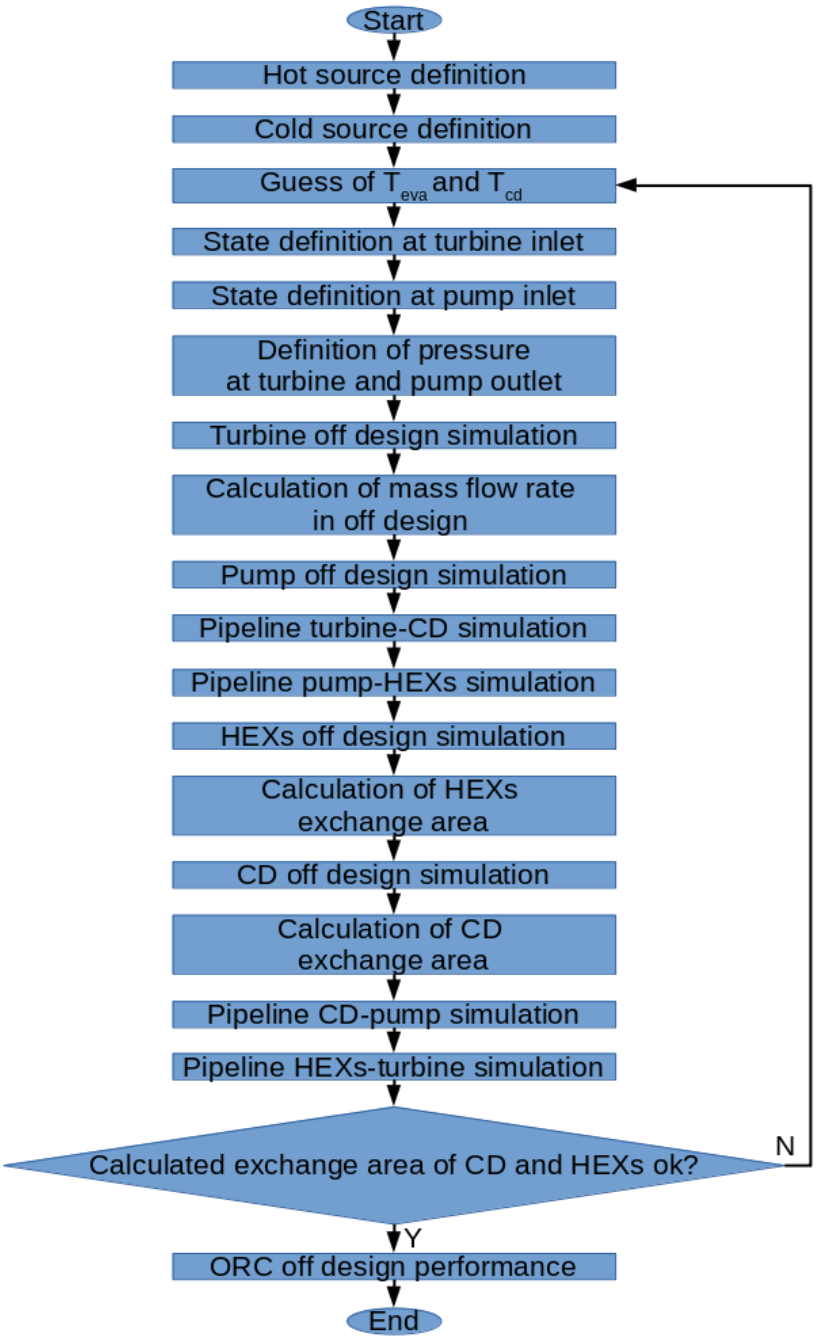

Figure 5: Algorithm of the ORC simulation model for off design

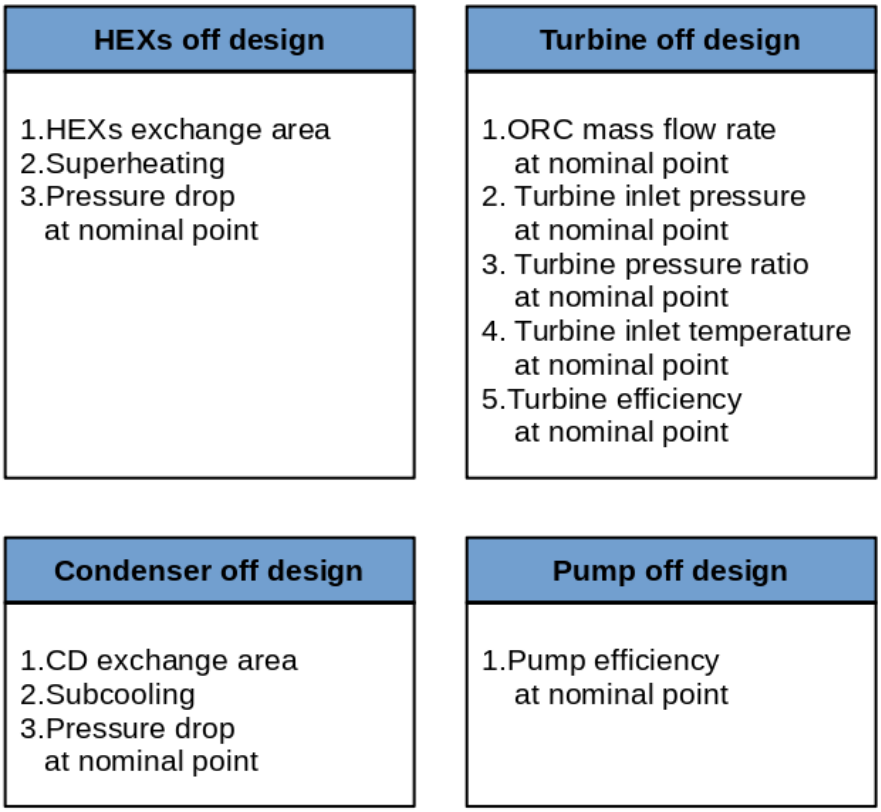

Figure 6: Input data for the simulation of the main components of the ORC in off design conditions

In the following, the deterministic ORC model is coupled with an uncertainty quantification method, described in the next section, to account for uncertainties in the nominal conditions.

3. ORC Uncertainty quantification

The goal of uncertainty quantification (UQ) is to estimate variability in the output of a model, corresponding to a set of Quantities of Interest (QoIs), given variations in the model inputs. Hereafter, we adopt a probabilistic approach which aims at predicting the probability density distributions of the output QoIs, given some probability distributions assigned to the inputs. For that purpose, a numerical algorithm is used to propagate the input PDFs through the model, here treated as a black box, leading to approximated PDF

(e.g., histograms) for the QoIs. This process is sketched in Fig.7.

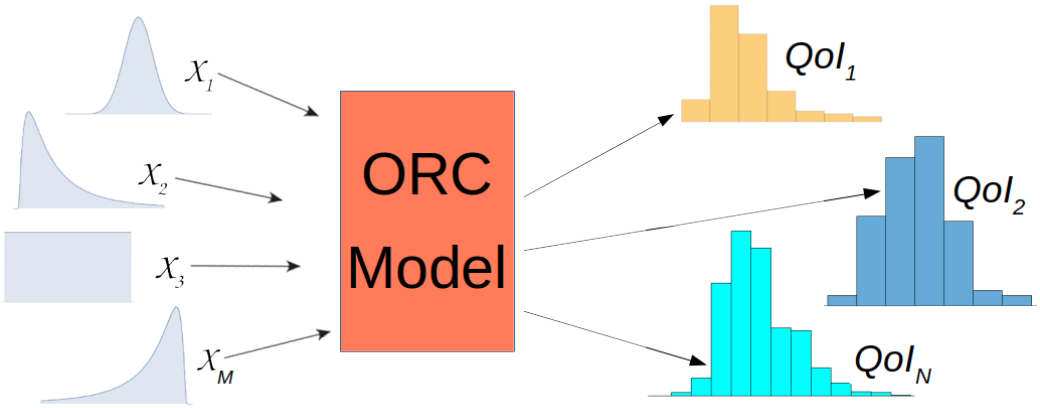

Figure 7: General sketch of the UQ process of the ORC

For the ORC model considered in the present work, the uncertain inputs are the operating conditions (hot and cold source characteristics) and the uncertain output QoIs are ORC performance parameters (i.e. cycle efficiency or power output) or ORC working characteristics, such as the mass flow rate. In the next Section, we discuss the selection of performance parameters that will serve as cost functions for the RDO.

3.1. Selection of the uncertain ORC performance parameters

The uncertain parameter selected in the present work as the target of the UQ algorithm and, subsequently, of the RDO strategy is the ORC net power, $W_{ORC,net}$. This is calculated as the difference of the electric power delivered by the generator and the sum of all consumption devices, namely, the feed pump and the auxiliaries like the cooling tower system, the oil system, the air compressors and the control room system. $W_{ORC,net}$ is here preferred to the global cycle efficiency, defined as the ratio of the ORC net power to the total heat content of the heat source: in fact, for a randomly varying thermal input, global efficiency does not necessarily correspond to the maximum power output operation of the ORC system. This happens because during the optimization, in case of an increase in the evaporation pressure, an increased cycle efficiency can be obtained at the cost of a decrease in the amount of heat extracted from the heat source. Therefore, instead of considering a possible trade-off between these two quantities, in the present study

we have chosen to work only with $W_{ORC,net}$, as it is an extensive quantity which is easier to be used in the optimization with respect to any possible constraint about the size of the plant.

To evaluate the influence of uncertain inputs on the selected QoI, the ORC model is first run in the design mode, with nominal conditions fixed to the average values of the input parameters. This allows to determine the geometrical characteristics of the ORC. Afterwards, the ORC model is run several times in the simulation mode for a set of conditions sampled from the input PDFs, and the corresponding values of the ouput QoI are used to build an approximation of its PDF and of its main statistical moments (mean and variance).

3.2. Identification of sources of uncertainty

The ORC system under investigation is affected by two major uncertainties: the first is of epistemic nature, as it is due to the lack of complete information about the characteristics of the geothermal heat source; the second one is aleatory and associated with the random variations of the temperature of the cold medium at the condenser.

About the first uncertainty, Sanyal and Morrow [11] conducted a local sensitivity study on the internal rate of return for a typical geothermal project, and illustrated that the most sensitive variables are resource parameters. Hereafter this uncertainty is considered as the outcome of the interaction of three sources of epistemic uncertainty, namely:

1. mass flow rate of the geothermal brine $\dot{m}_{geo}$,
2. temperature of the geothermal brine T_{geo},
3. heat capacity of the geothermal brine c_{geo}.

Based on information available in the technical literature (see for instance [42, 43, 44, 45]), the preceding quantities are modelled as independent Gaussian random variables, whose parameters are listed in Tab. 2.

Regarding the temperature of the cooling water T_{cw_in} at the inlet of the condenser, the observation of historical data could be used to infer a probability distribution modelling for this source of aleatory uncertainty. However, for the present work, no data were available; therefore, some information found in literature [45, 46] was used to model this quantity as a Gaussian random variable, with parameters also reported in Tab. 2.

Table 2: Parameters of ORC uncertain variables, modelled by Gaussian PDFs

Parameter	**Distribution**	**Mean**	**Variance**
$\dot{m}_{geo}$	Gaussian	162.0 kgs^{-1}	72.25 kg^2s^{-2}
T_{geo}	Gaussian	388.15 K	6.25 K^2
c_{geo}	Gaussian	4.2 $kJkg^{-1}K^{-1}$	0.0025 $kJ^2kg^{-2}K^{-2}$
T_{cw_in}	Gaussian	297.15 K	4 K^2

3.3. Uncertainty propagation

The objective of an UQ algorithm is to propagate input uncertainties through a model and estimate the PDF of output QoIs and/or their statistical moments. A large variety of UQ methods is available in the literature, the simplest and more general one being the Monte Carlo approach [47]. This consists in drawing samples from the input PDFs, and to compute for each of them the corresponding model outputs for the QoIs. The results may be used to construct an histogram of the output QoIs or to compute means and variances. Unfortunately, a very large number of samples is required to converge the statistics, which makes the Monte Carlo approach inapplicable to costly models. In [33] the Monte Carlo approach is successfully applied to the UQ and RDO of an ORC for automotive applications described through a simplified and inexpensive steady-state model, but a significant reduction of the number of samples is mandatory for extending its use to more realistic, complex models.

A way for alleviating the cost of uncertainty quantification is to project the system's response onto a suitable basis of analytical functions (often called a surrogate model) with coefficients estimated from a (possibly) small set of samples drawn from the costly model. The cheap surrogate is then used to evaluate Monte Carlo samples or to directly compute approximations of the statistical moments for the output quantities. An overview of UQ methods is out of the scope of this paper; examples can be found, e.g. in [48, 49, 50].

In the present work, we adopt a so-called Kriging surrogate model (see [51] for a review of Kriging methods). More specifically, a Bayesian Kriging surrogate is constructed from a design of experiments (DOE), which is a set of initial samples drawn from the simulation mode of the ORC model. The Kriging surrogate is used to approximate the behaviour of the costly ORC

model, and more specifically the response of the QoI to random variations of the uncertain inputs, as a cheap analytical function. The latter corresponds to the realization of a Gaussian process [52]. A detailed description of the Bayesian Kriging surrogate is beyond the scope of this paper. The interested reader is referred to Refs [53, 54, 55, 56] for more details. A proof of concept of Bayesian Kriging for the UQ of an ORC for waste heat recovery is available in [57].

Once the Bayesian Kriging surrogate has been trained on the DOE, a Monte Carlo sampling of the input PDF is carried out, as in the standard Monte Carlo method, and the QoI is evaluated for each sample using the analytical inexpensive surrogate instead of the full ORC model. The whole process can be summarized through the following steps:

1. Set the operating conditions to their average values, and run the ORC model in the design mode to determine the geometrical characteristics.
2. Build the DOE, by drawing a small set of samples, of size N, from the input PDF; these corresponds to multiple random combinations of the operating conditions.
3. For each sample, run the ORC model in simulation mode and determine the value of the QoI.
4. Use the data collected at points 2 and 3 to build the kriging surrogate function K: $\text{QoI} = K(\mathbf{X})$.
5. Draw a large set of samples, of size S, from the input PDF.
6. For each sample of point 5, compute the QoI from the kriging surrogate.
7. Use the results of point 6 to build an histogram of the QoI and/or to compute statistics (mean value of QoI, variance of QoI)

In the following calculations, the samples of point 2 are extracted by using the Latin Hypercube Sampling (LHS) criteria [58]. A preliminary accuracy study for a related case [57] has been here considered to select a number of Kriging samples providing the best tradeoff between cost and accuracy.

4. ORC optimization strategy

In order to design an ORC with a stable performance under the uncertain inputs, a RDO strategy is considered: the ORC model is coupled with an UQ method and an optimization algorithm to select design parameters that maximize (or depending on the problem, minimize) the expected (average)

value of a set of design criteria while optimizing some of their statistical properties, which are then added to the set of the cost functions.

In the following, we adopt the RDO criterion of Taguchi [30] which consists in optimizing the expectancy (statistical average) of some cost functions minimizing their variance at the same time.

More precisely, the following cost functions (CFs) are selected for the present work:

1. CF1 is the mean value of the PDF of the QoI ($E[W_{ORC,net}]$),
2. CF2 is the variance of the PDF of the QoI ($var[W_{ORC,net}]$),
3. CF3 is the global area of HEXs A_{ORC}.

The latter has been chosen as an indicator of the cost of the ORC: in fact, as a first approximation the cost of HEXs is proportional to their area, while the cost of components like the turbine and the pump is less sensitive to the design parameters as they benefit from a kind of economy of scale, due to the fact that the fix part of their cost is usually quite important and the variable part is usually proportional to their rated power. Consequently, the optimization problem has 3 objectives, which are the maximization of CF1, the minimization of CF2 and the minimization of CF3.

The design variables of the optimization process are the source characteristics $\dot{m}_{geo}$ and T_{geo} and the condensation temperature T_{cd}. Such parameters are uncertain, as discussed in the preceding sections. An additional design parameter, the superheating ΔT_{SH}, is also considered, and it is treated as deterministic. As an outcome of the UQ analysis performed (see results in Section 5), any other source of uncertainty, and namely c_{geo}, is neglected and the corresponding input parameters are set to their average values and assumed as deterministic.

The RDO algorithm, whose flowchart is depicted in Fig.8, proceeds as follows:

1. A nominal design point is randomly sorted from the input parameter distribution.
2. The ORC model is run in the design mode with deterministic inputs, determined at Point 1.
3. As an outcome of Point 2, the ORC characteristics are defined, including A_{ORC}.
4. The operating conditions are then randomly perturbed, according to their PDFs.

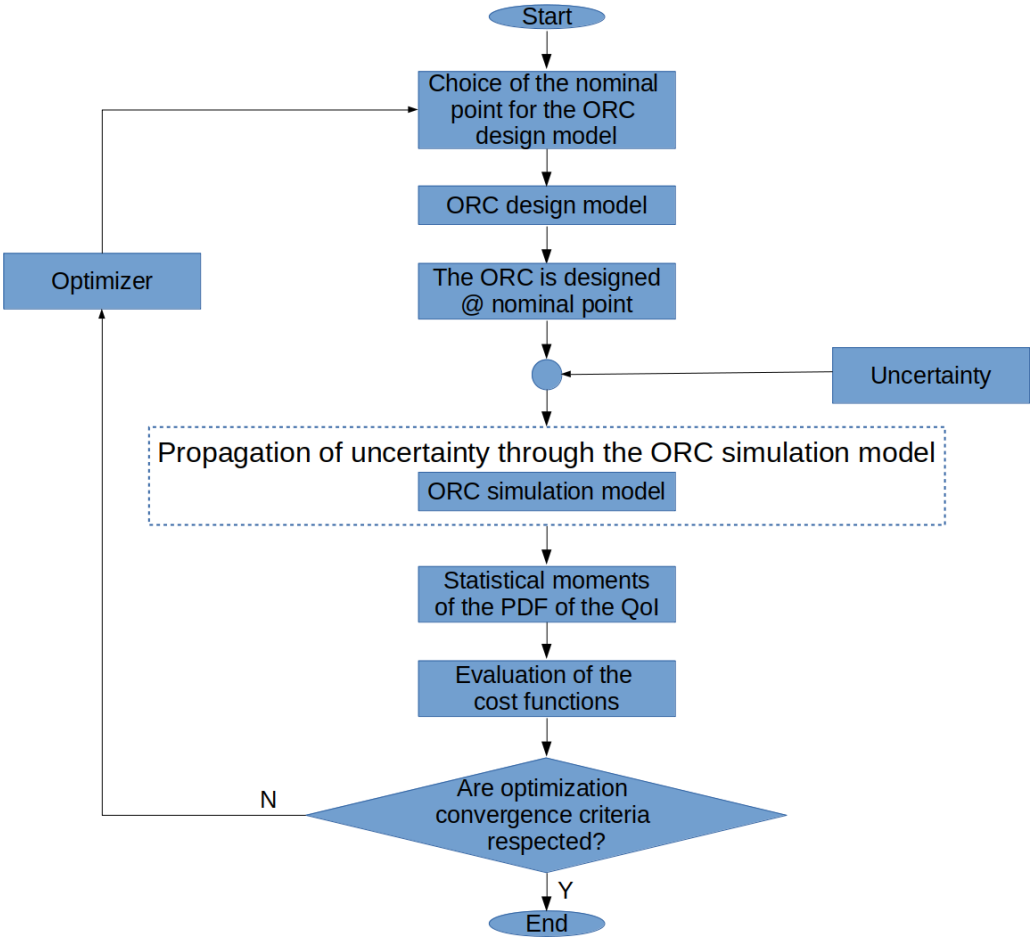

Figure 8: RDO simplified scheme

5. The random samples are propagated through the ORC model in simulation mode.
6. The cost functions CF1 and CF2 are evaluated as statistical moments of the QoI $W_{ORC,net}$.
7. Based on the values of the cost functions, a new set of design variables is selected and the process is repeated from Point 2.

In the present work, the optimizer is the multi-objective non-dominated sorting genetic algorithm (NSGAII) [59]. The design parameters space is defined by the support of the PDFs for the uncertain parameters and the interval [0, 4] K for ΔT_{SH}.

In the genetic algorithm, an initial population of 40 individuals (alternative nominal designs) is let to evolve over 80 generations. The evaluation of the cost functions for each individual corresponds to an UQ calculation, as described in Section 3. To alleviate the computational cost of the optimization process, the RDO is conducted by using two nested Bayesian Kriging (TNBK) surrogates, as in [56, 57].

The inner Kriging surrogate is used for UQ and the evaluation of CF1 and CF2, while the outer surrogate, describing variation of the CFs with the design parameters, is directly coupled with the optimizer. The workflow of the surrogate-based RDO, represented in Fig.9, proceeds as follows.

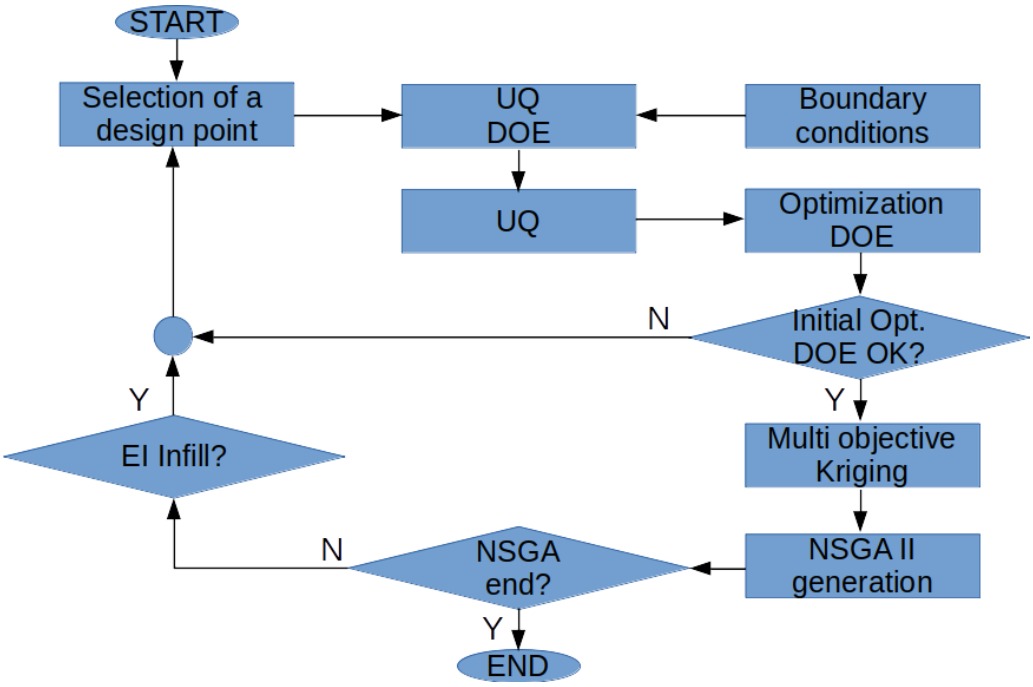

Figure 9: RDO detailed algorithm

1. An initial population, corresponding to 40 alternative design conditions is selected through LHS of the parameter space.
2. For each design, a UQ calculation is carried out based on the workflow in Fig. 8 and the cost functions are computed.
3. The external Bayesian Kriging relating the design variable to the cost functions, is constructed from the data collected at Point 1 and Point 2.

4. The NSGA II algorithm is run on the Kriging surrogate until convergence criteria are met.

In order to increase the accuracy of the external Kriging surrogate, during the NSGA II iterations an adaptive infill strategy based on the expected improvement (EI) criterion is used to add new samples to the initial set of data. Precisely, the infill procedure identifies a new design, whose cost functions are calculated with the full ORC model. The new point is then used to retrain the Kriging surface and the NSGA II is continued on the improved model. Based on numerical tests, we observed that applying an adaptive infill every 5 generations enables an accurate estimate of the optimal design. The cost functions of the optimal designs are finally recomputed exactly with the UQ solver in order to verify the residual errors.

5. UQ results and global sensitivity analysis

The sensitivity of the selected QoI, i.e. the ORC net power $W_{ORC,net}$, to random variations of the uncertain parameters described in Section 3.2 is first investigated by means of the UQ algorithm described above. The ORC model is first run in the design mode, with input parameters corresponding to the average values of Tab. 2. Afterwards, the ORC power output under random variation of the uncertain parameters is determined from a Bayesian Kriging surrogate of the ORC model in the simulation mode. More specifically, 50 LHS are drawn from the distribution of the uncertain parameters, and the resulting 50 sets of inputs are supplied to the ORC model to obtain the output $W_{ORC,net}$. A Bayesian Kriging surrogate of the output is then used to approximate the ORC model response for any value of the uncertain parameters. A set of 10^6 Monte Carlo samples is drawn from the input distributions and an approximation of $W_{ORC,net}$ is evaluated from the surrogate for each of them. These values are used to build a normalized histogram, reported in Fig. 10. We observe that the histogram follows closely a Gaussian distribution (also reported in the figure), with a standard deviation equal to approximately 14% of the mean value.

The UQ results are also used to carry out a global sensitivity analysis of the QoI to the uncertain parameters. For that purpose, we apply the analysis of variance (ANOVA) decomposition [60], and we use the Monte Carlo samples to estimate Sobol indexes [61] associated to the uncertain inputs. More specifically, for each input parameter we extract the first-order and

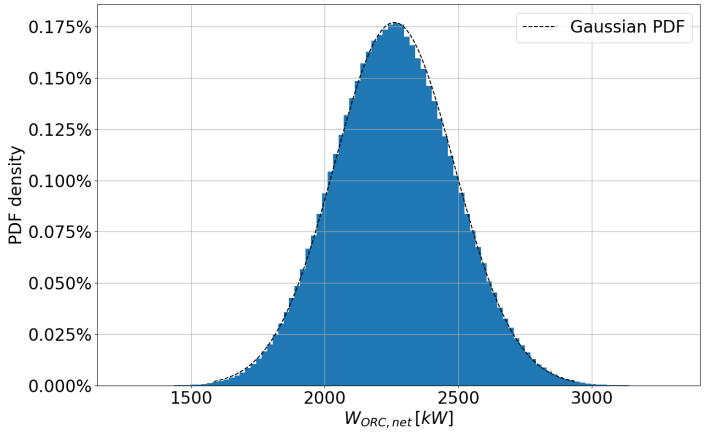

Figure 10: Histogram of the QoI $W_{ORC,net}$ under uncertainty

total Sobol indexes. The reader in referred to [62] for more details on Sobol global sensitivity analysis. Here we just recall that the first-order Sobol indexes measure the effect on the variance of the output QoI when perturbing each input parameter individually. The total Sobol indexes represent instead the overall contribution of a given input to the total variance of the output, when such a parameter is perturbed individually or in conjunction to other parameters. By construction, the Sobol indexes are numbers comprised between 0 and 1. Higher values indicate a stronger sensitivity of the QoI to a given parameter.

Table 3: Global sensitivity analysis with Sobol indexes

	Sobol 1st order	**Sobol Total**
$\dot{m}_{geo}$	17.6%	18.0%
T_{geo}	64.4%	64.7%
c_{geo}	0.40%	0.50%
T_{cd}	17.1%	17.4%

The results are reported in Tab.3 and Fig.11. The table shows that the first-order and total indexes are very close to each other, indicating that coupled effects due to the simultaneous variation of multiple inputs are small

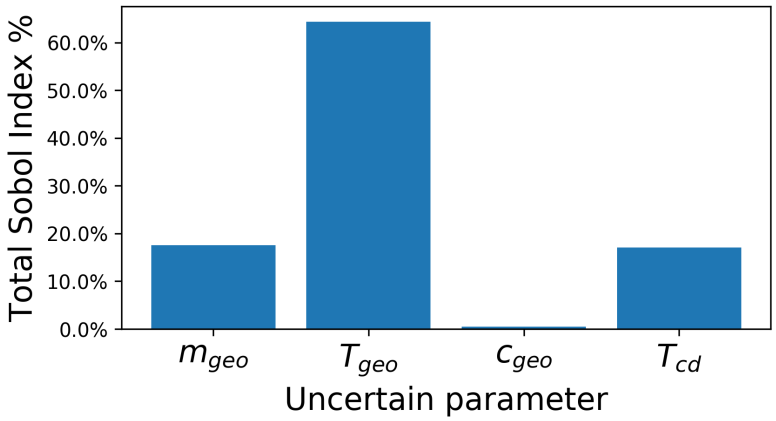

Figure 11: Total Sobol Index from Global sensitivity analysis

and that the system output is, to a good approximation, a linear function of the inputs. This is consistent with the Gaussian shape of the output PDF in Fig. 10 (a linear transformation of a Gaussian is a Gaussian). Fig.11 highlights the relative influence of the input parameters on the variance of the QoI $W_{ORC,net}$. The results show that the source temperature T_{geo} is by far the most important influential parameter. The brine mass flow rate $\dot{m}_{geo}$ and the condenser temperature T_{cd} also play a significant role, while the effect of c_{geo} can be neglected.

6. RDO results

The NSGA II algorithm allows to find an approximation of the Pareto front of sub-optimal solution, corresponding to different compromise solutions among the various objective. More precisely, the Pareto front is the subset of designs, for which all objective functions are equal or better than for all other designs. For the present RDO problem, the objective space has three dimensions and a graphical representation of the Pareto-optimal solutions is difficult. Fig.12 and Fig.13 show all the solutions computed by the NSGA II during the convergence process (blue dots) as well as the Pareto front (black line) in two dimensional subspaces. The cost functions are approximated from the Kriging surrogate.

Fig.12, corresponding to a scatter plot of CF2 versus CF1, shows a positive correlation between the first two cost functions, as the optimizer finds some design maximizing the mean value of the PDF of $W_{ORC,net}$, maximiz-

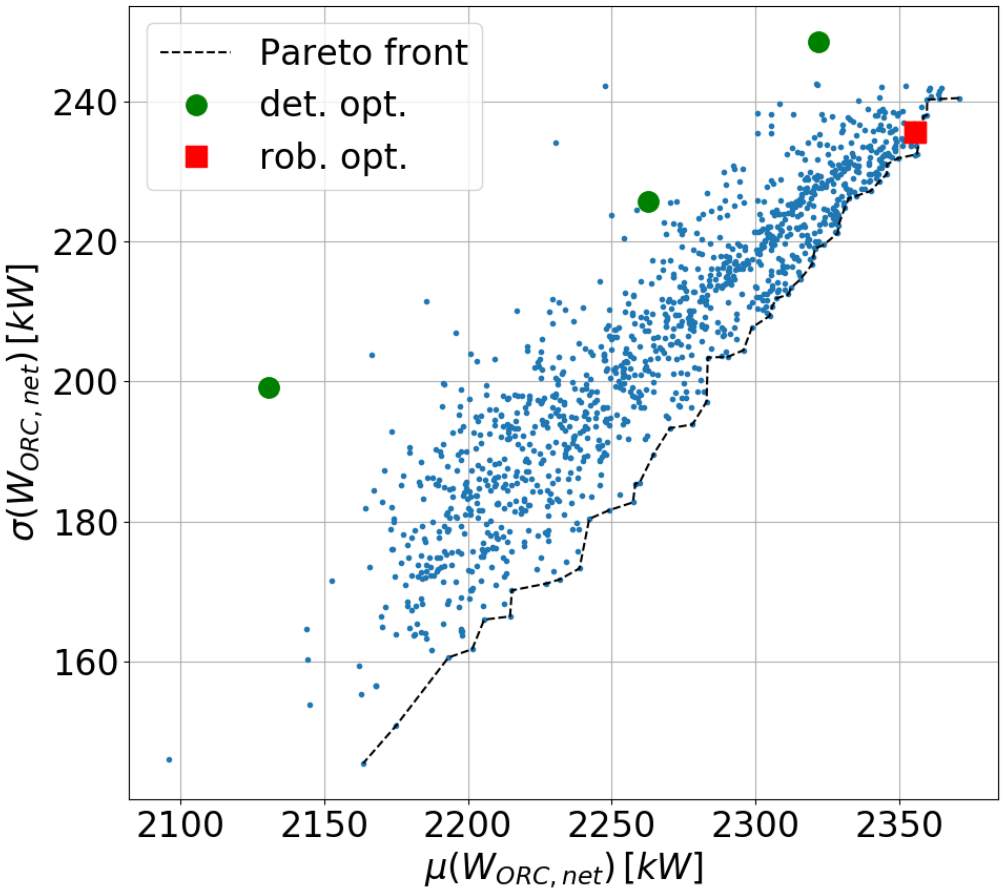

Figure 12: Objective space – CF1 vs CF2

ing at the same time its variance. Such a trend is also observed in Fig.13, where it appears that the maximization of the expected net power output corresponds to higher values of A_{ORC}. As a consequence, a unique optimum solution does not exist and different compromise solutions among the cost functions are possible.

Among all the designs lying on the Pareto front, we select the one offering the best trade-off among all optimization targets; the selected design is represented as a red symbol in Fig.12 and Fig.13 and it is identified by the parameters reported in Tab.4. The main characteristics of the final RDO design are listed in Tab.5.

The selected sub-optimal designs is input to the UQ solver, to verify the

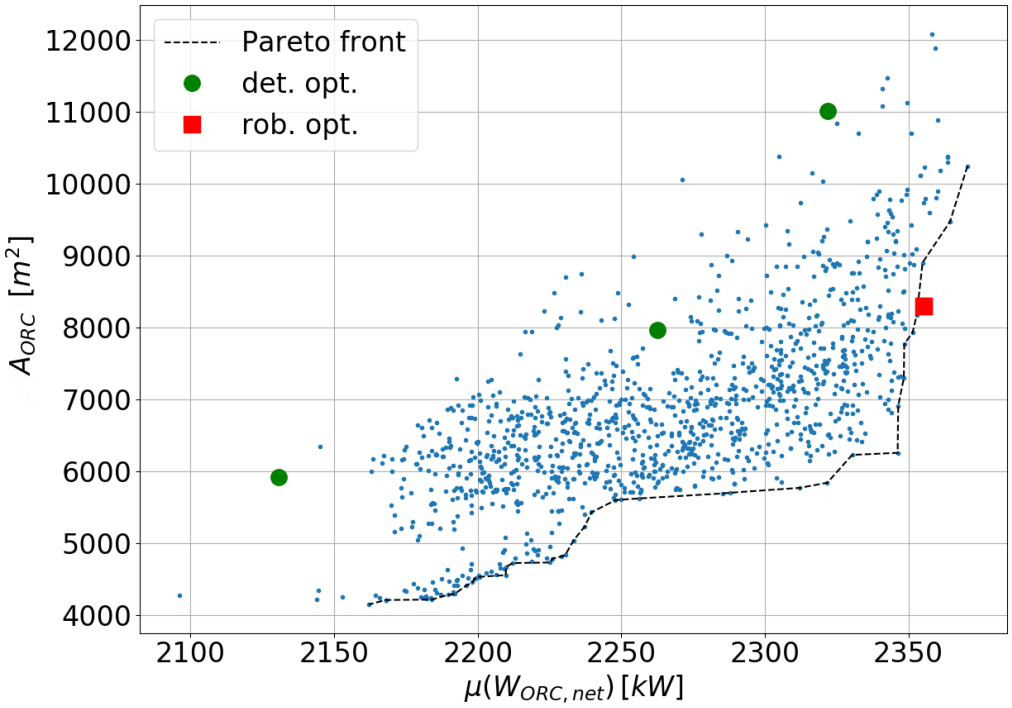

Figure 13: Objective space – CF1 vs CF3

Table 4: Optimal solution as a compromise of the optimization targets

$\dot{m}_{geo}$	T_{geo}	T_{cd}	ΔT_{SH}
148.1 kgs^{-1}	391.6 K	301.0 K	1.0 K

accuracy of the Kriging estimates of the cost functions by comparison with the full model. The distance between this solution and the line of the optimal solutions calculated with the TNBK approach, i.e. the surrogate approximation error, is found to be always lower than 5%. Despite this deviation, the selected design point outperforms the results of the deterministic optimization (green large dots in Fig.12 and Fig.13) carried out in three design points corresponding respectively to average, minimum and maximum conditions for the geothermal source, according to the PDFs in Tab.2.

Table 5: Optimal solution as a compromise of the optimization targets

Quantity	Unit	Value
ORC nominal mass flow rate	kgs^{-1}	61.1
ORC nominal evaporation pressure	bar	16.56
Superheating	K	1.0
Turbine nominal inlet pressure	bar	15.86
Turbine nominal outlet pressure	bar	4.70
ORC nominal condenser pressure	bar	4.60
ORC nominal thermal input	kW	23905.4
Turbine nominal mechanical power	kW	2491.3
Turbine nominal electric power	kW	2391.6
Pump nominal mechanical power	kW	189.4
ORC nominal net power	kW	2185.1
ORC nominal efficiency	-	9.1%
Heat exchangers total area	m^2	8297
Evaporator to Turbine pipe diameter	mm	500
Turbine to Condenser pipe diameter	mm	450
Condenser to Pump pipe diameter	mm	300
Pump to Evaporator pipe diameter	mm	300

7. Conclusions

A promising robust design optimization strategy based on two nested Bayesian kriging surrogates with an expected improvement infill approach has been successfully applied to an ORC for geothermal applications, affected both by epistemic and aleatory uncertainty. The first comes from the lack of information about the geothermal source and it is considered as the outcome of the interaction of the mass flow rate of the geothermal brine $\dot{m}_{geo}$, the temperature of the geothermal brine T_{geo}, and the heat capacity of the geothermal brine c_{geo}; on the other hand, the aleatory uncertainty is due to the yearly variation of the cooling water temperature at the condenser T_{cd}. Both these uncertainties can lead to an economic risk involving the whole geothermal project.

Before the RDO, a preliminary global sensitivity analysis has been carried out to evaluate the effect of the uncertain design parameters on the response

of the system; it turns out that the the most influential parameters are T_{geo}, $\dot{m}_{geo}$ and T_{cd}, while c_{geo} can be neglected. These results are used to reduce the number of optimization parameters that are considered in the RDO of the ORC.

From the analysis of the Pareto front, it comes out that a unique optimum solution does not exist and different compromise solutions among the cost functions are possible. Among them, the one offering the best trade-off among all optimization targets is selected. This optimal solution obtained with the RDO methodology is then compared with the optimal solutions from the deterministic optimization, which are always outperformed. In particular, the best RDO solution wins against the best deterministic optimum, increasing the mean value of the PDF of the QoI (the power production) by 1.5%, while its standard deviation is reduced by 8.5% and the surface of the heat exchangers by 34%.

Future work will focus on applying the present RDO methodology to more complex ORC configurations (for instance, recuperative cycles, multilevel cycles or systems with several pre-heaters in parallel), giving a focus also on operational aspects like failure probability.

References

[1] Bertani, R., Geothermal power generation in the world 2005–2010 update report, Geothermics 41 (2012) 1–29. doi:https://doi.org/10.1016/j.geothermics.2011.10.001.

[2] Bertani, R., Geothermal power generation in the world 2010–2014 update report, Geothermics 60 (2016) 31–43. doi:https://doi.org/10.1016/j.geothermics.2015.11.003.

[3] The International Renewable Energy Agency, Geothermal power: Technology brief, Tech. Rep. ISBN 978-92-9260-036-5 (PDF), IRENA, Abu Dhabi (Sep. 2017).

[4] Tartiere, T., Astolfi, M., A World Overview of the Organic Rankine Cycle Market, Energy Procedia 129 (2017) 2–9. doi:10.1016/j.egypro.2017.09.159.

[5] Barr, H., Grant, M.A., Coping With Uncertainty in Geothermal Field Development, Auckland University, 1984.

[6] American Institute of Aeronautics and Astronautics (Ed.), Guide for the Verification and Validation of Computational Fluid Dynamics Simulations, 1998.

[7] American Society of Mechanical Engineers, Standard for Verification and Validation in Computational Fluid Dynamics and Heat Transfer, ASME.

[8] A. Robertson-Tait, R. Henneberger, S. K. Sanyal, Managing Geothermal Resource Risk - Experience From the United States, Karlsruhe, Germany, 2008, p. 9.

[9] The World Bank - Energy Sector Management Assistance Program, Geothermal Handbook: Planning and Financing Power Generation, Tech. rep. (2012).

[10] S. K. Sanyal, J. B. Koenig, Resource risk and its mitigation for the financing of geothermal projects, in: Transactions International Geothermal Energy Conference, Florence, Italy, 1995, pp. 2911–2915.

[11] S. Sanyal, J. Morrow, Quantification of geothermal resource risk - A practical perspective, Transactions - Geothermal Resources Council 34 (2010) 117–122.

[12] Macchi, E., Astolfi, M., Organic Rankine Cycle Power Systems, Elsevier, 2017.

[13] Y. Dai, J. Wang, L. Gao, Parametric optimization and comparative study of organic Rankine cycle (ORC) for low grade waste heat recovery, Energy Conversion and Management 50 (3) (2009) 576–582. doi:10.1016/j.enconman.2008.10.018.

[14] Z. Q. Wang, N. J. Zhou, J. Guo, X. Y. Wang, Fluid selection and parametric optimization of organic Rankine cycle using low temperature waste heat, Energy 40 (1) (2012) 107–115. doi:10.1016/j.energy.2012.02.022.

[15] J. Wang, Z. Yan, M. Wang, S. Ma, Y. Dai, Thermodynamic analysis and optimization of an (organic Rankine cycle) ORC using low grade heat source, Energy 49 (2013) 356–365. doi:10.1016/j.energy.2012.11.009.

[16] J. Wang, Z. Yan, M. Wang, M. Li, Y. Dai, Multi-objective optimization of an organic Rankine cycle (ORC) for low grade waste heat recovery using evolutionary algorithm, Energy Conversion and Management 71 (2013) 146–158. doi:10.1016/j.enconman.2013.03.028.

[17] H. Xi, M. Li, C. Xu, Y. He, Parametric optimization of regenerative organic Rankine cycle (ORC) for low grade waste heat recovery using genetic algorithm, Energy 58 (2013) 473–482. doi:10.1016/j.energy.2013.06.039.

[18] L. Pierobon, T. Nguyen, U. Larsen, F. Haglind, B. Elmegaard, Multi-objective optimization of organic Rankine cycles for waste heat recovery: Application in an offshore platform, Energy 58 (2013) 538–549. doi:10.1016/j.energy.2013.05.039.

[19] J. G. Andreasen, U. Larsen, T. Knudsen, L. Pierobon, F. Haglind, Selection and optimization of pure and mixed working fluids for low grade heat utilization using organic Rankine cycles, Energy 73 (2014) 204–213. doi:10.1016/j.energy.2014.06.012.

[20] S. Lecompte, H. Huisseune, M. van den Broek, S. De Schampheleire, M. De Paepe, Part load based thermo-economic optimization of the Organic Rankine Cycle (ORC) applied to a combined heat and power (CHP) system, Applied Energy 111 (2013) 871–881. doi:10.1016/j.apenergy.2013.06.043.

[21] G. Manente, A. Toffolo, A. Lazzaretto, M. Paci, An Organic Rankine Cycle off-design model for the search of the optimal control strategy, Energy 58 (2013) 97–106. doi:10.1016/j.energy.2012.12.035.

[22] L. Pierobon, E. Casati, F. Casella, F. Haglind, P. Colonna, Design methodology for flexible energy conversion systems accounting for dynamic performance, Energy 68 (2014) 667–679. doi:10.1016/j.energy.2014.03.010.

[23] D. Maraver, J. Royo, V. Lemort, S. Quoilin, Systematic optimization of subcritical and transcritical organic Rankine cycles (ORCs) constrained by technical parameters in multiple applications, Applied Energy 117 (2014) 11–29. doi:10.1016/j.apenergy.2013.11.076.

[24] D. Walraven, B. Laenen, W. D'haeseleer, Optimum configuration of shell-and-tube heat exchangers for the use in low-temperature organic Rankine cycles, Energy Conversion and Management 83 (2014) 177–187. doi:10.1016/j.enconman.2014.03.066.

[25] U. Larsen, O. Sigthorsson, F. Haglind, A comparison of advanced heat recovery power cycles in a combined cycle for large ships, Energy 74 (2014) 260–268. doi:10.1016/j.energy.2014.06.096.

[26] D. Walraven, B. Laenen, W. D'haeseleer, Economic system optimization of air-cooled organic Rankine cycles powered by low-temperature geothermal heat sources, Energy 80 (2015) 104–113. doi:10.1016/j.energy.2014.11.048.

[27] E. Martelli, F. Capra, S. Consonni, Numerical optimization of Combined Heat and Power Organic Rankine Cycles – Part A: Design optimization, Energy 90 (2015) 310–328. doi:10.1016/j.energy.2015.06.111.

[28] F. Capra, E. Martelli, Numerical optimization of combined heat and power Organic Rankine Cycles – Part B: Simultaneous design & part-load optimization, Energy 90 (2015) 329–343. doi:10.1016/j.energy.2015.06.113.

[29] Beyer, H. G., Sendhoff, B., Robust optimization – A comprehensive survey, Computer Methods in Applied Mechanics and Engineering 196 (33) (2007) 3190–3218. doi:10.1016/j.cma.2007.03.003.

[30] Taguchi, G., System of experimental design: engineering methods to optimize quality and minimize costs, UNIPUB/Kraus International Publications, 1987.

[31] M. Maliki, B. Sudret, J. Bourinet, B. Guillaume, Quantile-based optimization under uncertainties using adaptive Kriging surrogate models, Structural and Multidisciplinary Optimization (May 2016). doi:10.1007/s00158-016-1504-4.

[32] L. Cook, J. Jarrett, Horsetail matching: a flexible approach to optimization under uncertainty (May 2017). doi:10.17863/CAM.9396.

[33] E. A. Bufi, S. M. Camporeale, P. Cinnella, Robust optimization of an Organic Rankine Cycle for heavy duty engine waste

heat recovery, Energy Procedia 129 (Supplement C) (2017) 66–73. doi:10.1016/j.egypro.2017.09.190.

[34] F. Fontaine, Design and Simulation Model of Medium Scale Organic Rankine Cycles - Validation on Waste Heat Recovery Plant and Case Studies, MS Thesis, University of Liege (Sept. 2018).

[35] I. H. Bell, S. Quoilin, E. Georges, J. E. Braun, E. A. Groll, W. T. Horton, V. Lemort, A generalized moving-boundary algorithm to predict the heat transfer rate of counterflow heat exchangers for any phase configuration, Applied Thermal Engineering 79 (2015) 192 – 201. doi:https://doi.org/10.1016/j.applthermaleng.2014.12.028.

[36] F. P. Incropera, D. P. DeWitt, T. L. Bergman, A. S. Lavine, Fundamentals of Heat and Mass Transfer, 6th Edition, Wiley, 2007, google-Books-ID: _P9QAAAAMAAJ.

[37] I. H. Bell, J. Wronski, S. Quoilin, V. Lemort, Pure and pseudo-pure fluid thermophysical property evaluation and the open-source thermophysical property library coolprop, Industrial & Engineering Chemistry Research 53 (6) (2014) 2498–2508. arXiv:http://pubs.acs.org/doi/pdf/10.1021/ie4033999, doi:10.1021/ie4033999.

[38] J. A. Nelder, R. Mead, A simplex method for function minimization, Comput. J. 7 (1965) 308–313.

[39] P. Virtanen, R. Gommers, T. E. Oliphant, M. Haberland, T. Reddy, D. Cournapeau, E. Burovski, P. Peterson, W. Weckesser, J. Bright, S. J. van der Walt, M. Brett, J. Wilson, K. Jarrod Millman, N. Mayorov, A. R. J. Nelson, E. Jones, R. Kern, E. Larson, C. Carey, İ. Polat, Y. Feng, E. W. Moore, J. Vand erPlas, D. Laxalde, J. Perktold, R. Cimrman, I. Henriksen, E. A. Quintero, C. R. Harris, A. M. Archibald, A. H. Ribeiro, F. Pedregosa, P. van Mulbregt, S. . . Contributors, SciPy 1.0: Fundamental Algorithms for Scientific Computing in Python, Nature Methods 17 (2020) 261–272. doi:https://doi.org/10.1038/s41592-019-0686-2.

[40] C. F. Colebrook, C. M. White, G. I. Taylor, Experiments with fluid friction in roughened pipes, Proceedings of the Royal Society of London.

Series A - Mathematical and Physical Sciences 161 (906) (1937) 367–381. doi:10.1098/rspa.1937.0150.

[41] M. Powell, A view of algorithms for optimization without derivatives, Mathematics TODAY 43 (01 2007).

[42] C. Vogt, D. Mottaghy, V. Rath, A. Wolf, R. Pechnig, C. Clauser, Quantifying Uncertainty in Geothermal Reservoir Modeling, Proceedings World Geothermal Congress (2010) 25–29.

[43] A. Foerster, Analysis of borehole temperature data in the Northeast German Basin: Continuous logs versus bottom-hole temperatures, Petroleum Geoscience 7 (2001) 241–254. doi:10.1144/petgeo.7.3.241.

[44] Y. Lee, D. Deming, K. Chen, Heat flow and heat production in the Arkoma Basin and Oklahoma Platform, southeastern Oklahoma, Journal of Geophysical Research 101 (1996) 25387–25401. doi:10.1029/96JB02532.

[45] H. J. Olsen, Geothermal reservoir assessment based on slim hole drilling, Electric Power Research Institute, 1993.

[46] Ashrae, Ashrae Handbook 2016: HVAC Systems and Equipment: SI Edition, ASHRAE Handbook of Heating, Ventilating and Air-Conditioning Systems and Equipment SI, ASHRAE, 2016.

[47] G. Fishman, Monte Carlo - Concepts, Algorithms, and Applications, Springer, 1996.

[48] P. Cinnella, S. J. Hercus, Robust optimization of dense gas flows under uncertain operating conditions, Computers & Fluids 39 (10) (2010) 1893–1908. doi:10.1016/j.compfluid.2010.06.020.

[49] W. N. Edeling, R. P. Dwight, P. Cinnella, Simplex-stochastic collocation method with improved scalability 310 301–328. doi:10.1016/j.jcp.2015.12.034.

[50] K. Tang, P. M. Congedo, R. Abgrall, Adaptive surrogate modeling by ANOVA and sparse polynomial dimensional decomposition for global sensitivity analysis in fluids simulation, Journal of Computational Physics 314 (2015) 36.

[51] A. Forrester, A. Sobester, A. Keane, Engineering Design via Surrogate Modelling: A Practical Guide, John Wiley & Sons, 2008.

[52] C. E. Rasmussen, C. K. I. Williams, Gaussian Processes for Machine Learning, The MIT Press, Cambridge, Mass, 2006.

[53] M. C. Kennedy, A. O'Hagan, Bayesian Calibration of Computer Models, Journal of the Royal Statistical Society, Series B, Methodological 63 (2000) 425–464.

[54] C. K. Wikle, L. M. Berliner, A Bayesian tutorial for data assimilation, Physica D: Nonlinear Phenomena 230 (1) (2007) 1–16. doi:10.1016/j.physd.2006.09.017.

[55] De Baar, J.H.S., Stochastic Surrogates for Measurements and Computer Models of Fluids, Ph.D. thesis (2014).

[56] E. A. Bufi, P. Cinnella, Robust optimization of supersonic ORC nozzle guide vanes, J. Phys.: Conf. Ser. 821 (1) (2017) 012014. doi:10.1088/1742-6596/821/1/012014.

[57] A. Serafino, B. Obert, H. Hagi, P. Cinnella, Assessment of an Innovative Technique for the Robust Optimization of Organic Rankine Cycles, American Society of Mechanical Engineers Digital Collection, 2019. doi:10.1115/GT2019-90170.

[58] M. D. McKay, R. J. Beckman, W. J. Conover, Comparison of three methods for selecting values of input variables in the analysis of output from a computer code, Technometrics 21 (2) (1979) 239–245. arXiv:https://doi.org/10.1080/00401706.1979.10489755, doi:10.1080/00401706.1979.10489755.

[59] K. Deb, A. Pratap, S. Agarwal, T. Meyarivan, A fast and elitist multiobjective genetic algorithm: NSGA-II 6 (2) 182–197. doi:10.1109/4235.996017.

[60] R. Liu, A. B. Owen, Estimating mean dimensionality of analysis of variance decompositions, Journal of the American Statistical Association 101 (474) (2006) 712–721.

[61] R. Ballester-Ripoll, E. G. Paredes, R. Pajarola, Sobol tensor trains for global sensitivity analysis, Reliability Engineering and System Safety 183 (2019) 311 – 322. doi:https://doi.org/10.1016/j.ress.2018.11.007.

[62] I. Sobol, Global sensitivity indices for nonlinear mathematical models and their monte carlo estimates 55 (1) 271–280. doi:10.1016/S0378-4754(00)00270-6.